Communication: Water activation and splitting by single metal-atom anions

Gaoxiang Liu, Evangelos Miliordos, Sandra M. Ciborowski, Martin Tschurl, Ulrich Boesl, Ulrich Heiz, Xinxing Zhang, Sotiris S. Xantheas, and Kit Bowen

Citation: J. Chem. Phys. **149**, 221101 (2018); doi: 10.1063/1.5050913
View online: https://doi.org/10.1063/1.5050913
View Table of Contents: http://aip.scitation.org/toc/jcp/149/22
Published by the American Institute of Physics

Communication: Water activation and splitting by single metal-atom anions

Gaoxiang Liu,[1] Evangelos Miliordos,[2,a)] Sandra M. Ciborowski,[1] Martin Tschurl,[3] Ulrich Boesl,[3] Ulrich Heiz,[3] Xinxing Zhang,[4,b)] Sotiris S. Xantheas,[2,5,b)] and Kit Bowen[1,b)]
[1]*Department of Chemistry, Johns Hopkins University, Baltimore, Maryland 21218, USA*
[2]*Advanced Computing, Mathematics and Data Division, Pacific Northwest National Laboratory, Richland, Washington 99354, USA*
[3]*Institute for Physical Chemistry, Technical University of Munich, 85748 Garching, Germany*
[4]*Key Laboratory of Advanced Energy Materials Chemistry (Ministry of Education), College of Chemistry, Nankai University, Tianjin 30071, China*
[5]*Department of Chemistry, University of Washington, Seattle, Washington 98195, USA*

(Received 3 August 2018; accepted 22 October 2018; published online 10 December 2018)

We report experimental and computational results pertaining to the activation and splitting of single water molecules by single atomic platinum anions. The anion photoelectron spectra of $[Pt(H_2O)]^-$, formed under different conditions, exhibit spectral features that are due to the anion-molecule complex, $Pt^-(H_2O)$, and to the reaction intermediates, $HPtOH^-$ and H_2PtO^-, in which one and two O–H bonds have been broken, respectively. Additionally, the observations of PtO^- and H_2^+ in mass spectra strongly imply that water splitting via the reaction $Pt^- + H_2O \rightarrow PtO^- + H_2$ has occurred. Extending these studies to nickel and palladium shows that they too are able to activate single water molecules, as evidenced by the formation of the reaction intermediates, $HNiOH^-$ and $HPdOH^-$. Computations at the coupled cluster singles and doubles with perturbatively connected triples level of theory provide structures and vertical detachment energies (VDEs) for both $HMOH^-$ and H_2MO^- intermediates. The calculated and measured VDE values are in good agreement and thus support their identification. *Published by AIP Publishing.* https://doi.org/10.1063/1.5050913

INTRODUCTION

Water splitting holds great promise as a source of clean, abundant fuel.[1–5] While electrolysis is effective, its cost is exceedingly high. Likewise, the direct cleavage of water's O–H bond is energetically prohibitive (497.1 kJ/mol).[6] The solution to this problem is generally thought to lie in catalytic water splitting, a process which depends critically on the activation of water molecules. A variety of molecular and cluster catalysts are known to be effective in aqueous media,[7,8] on surfaces,[9,10] and in gas phase environments.[11,12] Single-atom catalysts provide yet another approach. While single-atom catalysts have been found to facilitate water splitting on surfaces,[13–16] water activation and splitting by single atoms in the gas phase have gone virtually unexplored. Here, we investigate this topic, addressing both water activation and water splitting by single metal atomic anions.

We had originally been inspired by experiments in which sub-nano-size platinum clusters deposited onto semiconductor nano-rods and submerged in water were found to be effective water splitting photocatalysts.[17–19] There, the overall catalytic process was $H_2O + Pt_n^- = ½\ H_2 + Pt_n + OH^-$. Rather than studying water activation by platinum *cluster* anions, however, we chose to focus on the simplest set of relevant reactants, i.e., a *single* water molecule, a *single* metal atom (M), and a *single* excess electron (e^-), all interacting together within the sub-nano crucible of gas phase $[M(H_2O)]^-$ cluster anions. By extending these studies beyond platinum to include nickel and palladium, as well as several other transition metal atoms, we explored the activation and splitting of single water molecules by single atomic metal anions. Our joint experimental and theoretical effort has resulted in strong evidence for both water activation and water splitting by single atomic platinum anions and for water activation (but without splitting) by single nickel and palladium anions.

RESULTS AND DISCUSSIONS

Experimental studies of $[Pt(H_2O)]^-$ were conducted using a laser vaporization ion source, time-of-flight (TOF) mass spectrometry, and anion photoelectron spectroscopy.[20] Source details are presented in the supplementary material. The left panels in Fig. 1 present the mass spectra of the $[Pt(H_2O)]^-$ mass region along with the expected isotopic mass distribution pattern of $[Pt(H_2O)]^-$ in its top panel. Mass spectra **A**, **B**, and **C** show the effect of increasing the vaporization laser power in three steps (6, 8, and 11 mJ). Note that mass peaks due to PtO^- appeared and became stronger with increasing power. Control experiments without water, but under the same vaporization laser power conditions, did not result in the formation of PtO^- (Fig. S1), suggesting that PtO^- had formed as

a)Present address: Department of Chemistry and Biochemistry, Auburn University, Auburn, AL 36830, USA.
b)Authors to whom correspondence should be addressed: kbowen@jhu.edu; sotiris.xantheas@pnnl.gov; and idea.then.diligence@gmail.com

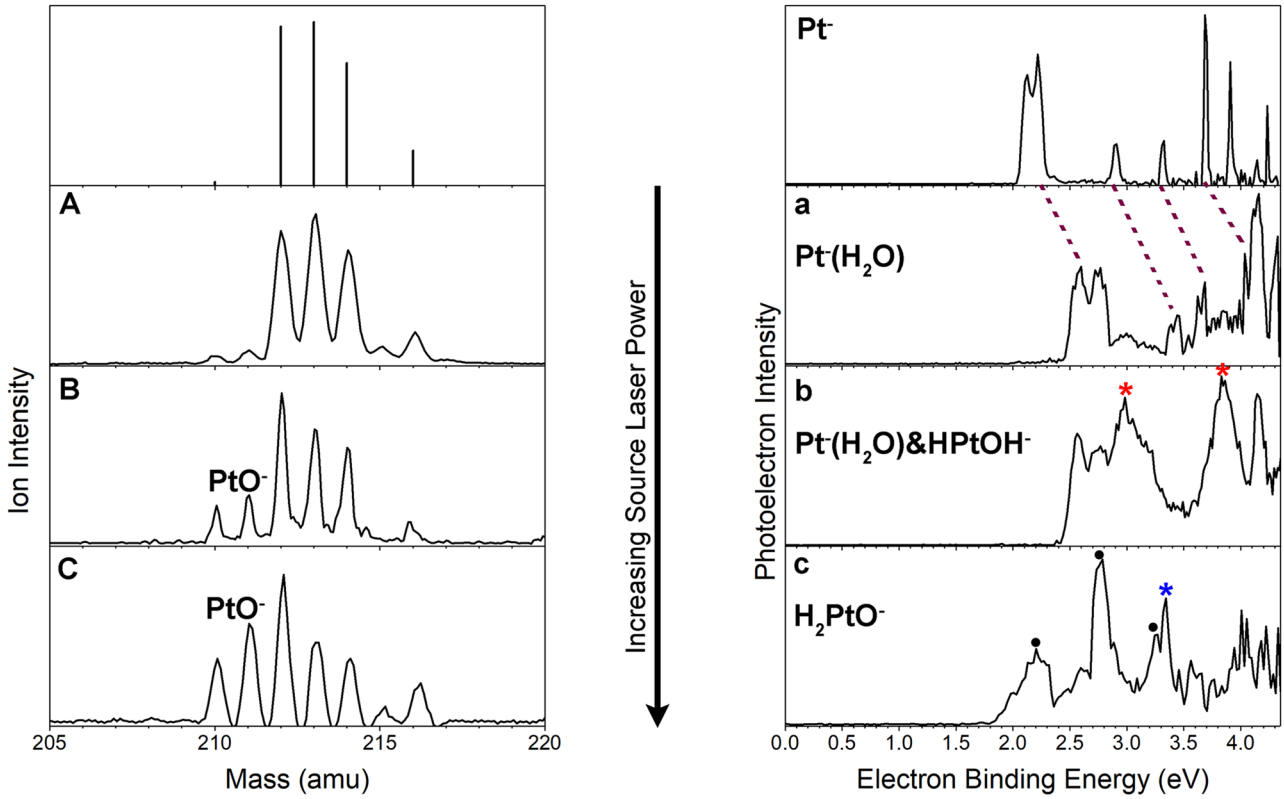

FIG. 1. The top left panel presents a stick mass spectrum showing the simulated isotopic mass distribution of $[Pt(H_2O)]^-$. The panels below it show the mass spectra of $[Pt(H_2O)]^-$ species formed under three different laser vaporization power source conditions; mass spectrum **A** was recorded under low vaporization laser power, **B** under moderate vaporization laser power, and **C** under high vaporization laser power. In all cases, laser vaporization was carried out using the second harmonic (2.33 eV/photon) of a Nd:YAG laser. The top right panel presents the anion photoelectron spectrum of the Pt^- atomic anion. The panels below it show the anion photoelectron spectra of $[Pt(H_2O)]^-$ species **a**, **b**, and **c**, where in each case the $[Pt(H_2O)]^-$ anions had been generated under the same laser vaporization power conditions used to record their corresponding mass spectra **A**, **B**, and **C**, respectively. In all cases, the anion photoelectron spectra were measured using the fourth harmonic (4.66 eV/photon) of a Nd:YAG laser.

a result of the reaction between Pt^- and H_2O. The identities of the two putative PtO^- mass peaks (m = 210 and 211) were confirmed by measuring their anion photoelectron spectra (see Fig. S2) and comparing them to a previous report.[21] The fact that the anion photoelectron spectra at these two masses were identical also indicates that no $PtOH^-$ was present in the beam, since it would have appeared at m = 211.

The top panel on the right-hand side of Fig. 1 presents the photoelectron spectrum of the platinum atomic anion, Pt^-. This spectrum is presented for reference and agrees with previous reports.[22] The lower three panels on the right-hand side of Fig. 1 exhibit anion photoelectron spectra of $[Pt(H_2O)]^-$, i.e., **a**, **b**, and **c**, where in each case the subject $[Pt(H_2O)]^-$ species had been generated under the same laser vaporization (source) power conditions that had been used to measure their corresponding mass spectra **A**, **B**, and **C**, respectively. All $[Pt(H_2O)]^-$ spectra were taken at mass = 216 to ensure that the photoelectron signals were solely from $[Pt(H_2O)]^-$. These three photoelectron spectra of $[Pt(H_2O)]^-$ clearly differ substantially from one another, strongly suggesting the presence of $[Pt(H_2O)]^-$ isomers, whose generation depended on laser vaporization (source) power. As will be explained below, the anion photoelectron spectra **a**, **b**, and **c** have been labeled with the identities of their $[Pt(H_2O)]^-$ isomers.

Potentially, the anionic metal-water complex, $[M(H_2O)]^-$, could exist in three different structures: (i) one in which M^- is "solvated" by a physisorbed water molecule, resulting in $M^-(H_2O)$, (ii) a structure where one of the O–H bonds in H_2O has been broken, resulting in $HMOH^-$, and (iii) a structure in which both O–H bonds in H_2O have been broken, resulting in H_2MO^-. As we will show, all three of these structural isomers were found to exist in the ion beam. The anionic complexes that result from one or both O–H bonds having been broken and the detached atom(s) having been reattached are water activation products. These activated species are *intermediates* along the reaction pathway that leads to H_2 formation, i.e., water splitting.

We utilized anion photoelectron spectroscopy to distinguish between these isomers.[23] Typically, when weak physisorption ("solvation") interactions occur between an anion and a water molecule, i.e., in anion-molecule complexes, the photoelectron spectral pattern of the resulting hydrated anion closely resembles that of the anion alone, except for it having been shifted to slightly higher electron binding energy (EBE) values and its features broadened. This is because M^- remains the chromophore for photodetachment; no truly chemical interactions have occurred. Photoelectron spectrum **a** on the right-hand side of Fig. 1 is an example of such an interaction. Its spectrum displays the same spectral pattern as the photoelectron spectrum of Pt^-, which sits above it in Fig. 1, except for its peaks being slightly blue-shifted and broadened. The $[Pt(H_2O)]^-$ isomer in photoelectron spectrum **a** is

thus seen to be the platinum atomic anion-water "solvation" complex, $Pt^-(H_2O)$.

At higher laser vaporization (source) power, PtO^- begins to appear in mass spectrum **B** of Fig. 1. Photoelectron spectrum **b** exhibits both the hydrated anion spectral peaks of spectrum **a** and new features, the most prominent of which are marked with red stars at EBE values of 2.98 eV and 3.83 eV. This new feature is due to another (a second) isomer.

At still higher laser vaporization (source) power, mass peaks due to PtO^- in mass spectrum **C** have become even stronger. In its corresponding anion photoelectron spectrum, i.e., **c**, the peaks due to the solvated anion, $Pt^-(H_2O)$, have completely disappeared and four new peaks have appeared. One of them, marked with a blue star at EBE = 3.34 eV, is due to yet another, i.e., a third, isomer of $[Pt(H_2O)]^-$, while the other three peaks, marked with black dots, exhibit EBE values that are identical to those in the photoelectron spectrum of PtO^- [see Fig. S2 and Ref. 21]. There are two possible explanations for the appearance of the PtO^- photoelectron spectrum within photoelectron spectrum **c**: (1) These peaks may have arisen due to two-photon processes, in which the first photon dissociated the newly formed, third $[Pt(H_2O)]^-$ isomer, producing PtO^-, while a second photon photodetached an electron from PtO^-. (2) Due to the relatively high source-laser power being used in this case, another possibility is that metastable $[Pt(H_2O)]^-$ was formed in the source and that it dissociated along the time-of-flight drift path, resulting in PtO^-, which continued to travel at the velocity of the TOF-extracted $[Pt(H_2O)]^-$ anions into the photodetachment region.[24] Since photoelectron spectrum **c** was taken at the unambiguous mass of $[Pt(H_2O)]^-$, this evidence alone implies that the newly formed (third) isomer in photoelectron spectrum **c** must have been H_2PtO^- and that the other fragment must have been H_2. Together, anion photoelectron spectra **a**, **b**, and **c** thus revealed the presence of three structural isomers of $[Pt(H_2O)]^-$, the hydrated Pt^- anion complex and two others, both of which involved O–H bond breaking.

Normally, the neutral products of a gas-phase reaction can only be indirectly deduced by counting the atom difference between reactants and charged products. Here, however, to search for the presence of H_2, which had been implied by our observations, we utilized an electron bombardment ionizer located along the beam path between the source and the TOF ion extractor. There, we changed appropriate voltages and polarities in order to record positive ion mass spectra so that neutral H_2 could be ionized to H_2^+ and observed by our mass spectrometer. Nevertheless, when the laser vaporization (source) power was low, no H_2^+ was seen. The only cations that we observed were He^+, O^+, OH^+, and H_2O^+ as seen in Fig. 2(a), all of which had formed due to ionization of H_2O/He backing gases from the source. However, when the laser power was increased to the level used to record mass spectrum **C**, H_2^+ was detected as shown in Fig. 2(b). This observation provided direct evidence that a single platinum atomic anion reacting with a single water molecule had produced H_2.

The photoelectron spectra of $[Pt(H_2O)_2]^-$ and $[Pt(H_2O)_3]^-$ are presented in Fig. S3. The absence of new features in these spectra suggests that when Pt^- reacts with either a water dimer or trimer, it only interacts with a single water molecule, while the other water molecules just solvate the $[Pt(H_2O)^-]$.

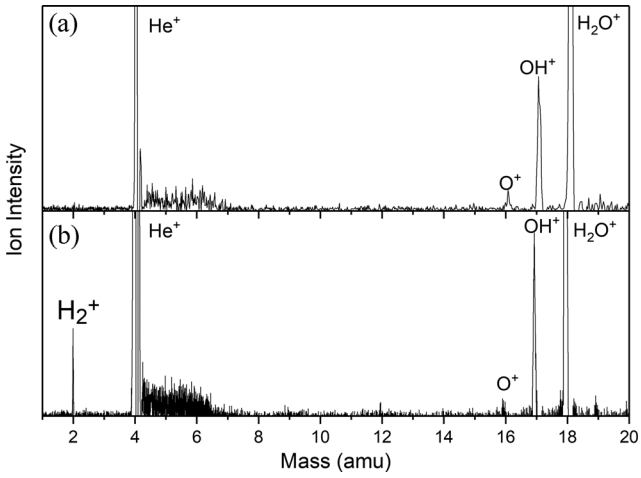

FIG. 2. Positive ion, electron bombardment ionization mass spectra of the species made under low vaporization laser power (a) and high vaporization laser power (b).

Parallel experimental studies were also conducted on $[Ni(H_2O)]^-$ and $[Pd(H_2O)]^-$. Their experimental mass spectra are presented in Fig. S4, along with their expected isotopic mass distributions. Unlike in the case of $[Pt(H_2O)]^-$, neither NiO^- nor PdO^- was observed even at elevated source laser powers. Additionally, no H_2^+ was observed in either of these cases, indicating that H_2 was not formed. Figure 3 presents the anion photoelectron spectra of $[Ni(H_2O)]^-$ and $[Pd(H_2O)]^-$, along with those of their corresponding atomic anions, Ni^- and Pd^-. As in anion photoelectron spectrum **b**, in the case of $[Pt(H_2O)]^-$, the photoelectron spectra of $[Ni(H_2O)]^-$ and $[Pd(H_2O)]^-$ exhibit spectral features that are due to both the solvated anion complexes, $Ni^-(H_2O)$ and $Pd^-(H_2O)$, and additional structural isomers, these being marked by red dots in Fig. 3. As will be explained below, the anion photoelectron spectra of $[Ni(H_2O)]^-$ and $[Pd(H_2O)]^-$ have been labeled with the identities of their isomers.

In addition to measuring the anion photoelectron spectra of $[M(H_2O)]^-$, where M = Pt, Ni, and Pd, we also measured the photoelectron spectra of $[M(H_2O)]^-$, where M = Cu, Ag, Au, Fe, Co, and V. These latter $[M(H_2O)]^-$ species were formed utilizing the same source laser power protocol used to make $[Ni(H_2O)]^-$ and $[Pd(H_2O)]^-$ and photoelectron spectrum **b** in the case of $[Pt(H_2O)]^-$. The anion photoelectron spectra of $[M(H_2O)]^-$, where M = Cu, Ag, Au, Fe, Co, and V, are displayed along with their atomic anion photoelectron spectra in Fig. S5. All of them are simple anion-molecule (physisorbed) complexes, i.e., $M^-(H_2O)$. It is important to note that none of them showed any photoelectron spectral features beyond those expected for an anion-molecule complex.

The details of our computational methods are presented in the supplementary material. Briefly, to assess the potential multi-reference nature of $[M(H_2O)]^-$ and its neutral counterparts, we initially relied on the internally contracted Multi-Reference Configuration Interaction (icMRCI) level of theory. The resultant mainly single reference character implied by those icMRCI calculations allowed us to employ the size-extensive, coupled cluster singles and doubles with

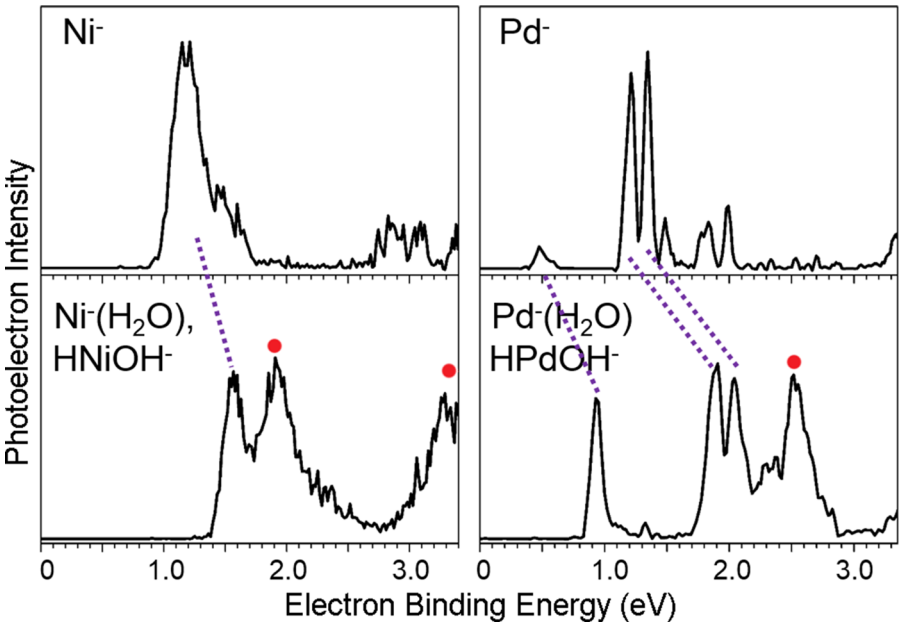

FIG. 3. Photoelectron spectra of the atomic metal anions, M^-, (in the upper panels) and their corresponding $[M(H_2O)]^-$ anions (in the lower panels), where M = Ni and Pd. All of these anion photoelectron spectra were measured using the third harmonic (3.49 eV/photon) of a Nd:YAG laser. Dotted tie-lines link M^- peaks to the corresponding blue-shifted peaks in their $M^-(H_2O)$ anion-molecule complexes. Additional structural isomers are marked by red dots.

perturbatively connected triples [CCSD(T)] approach to calculate vertical detachment energies (VDEs), where VDE is the vertical energy difference between an anion's ground state and its neutral counterpart at the structure of the anion.

The EBE values of the peak maxima in the photoelectron spectra are their VDE values. We have calculated VDE values for both $HMOH^-$ and H_2MO^- isomers (M = Pt, Ni, Pd) and compared them with the measured VDE values of the new spectral features. These are presented in Table I. For the $HMOH^-$ isomer, good agreement was obtained between experimental and calculated VDE values, indicating that the water-activated isomers, $HPtOH^-$, $HNiOH^-$, and $HPdOH^-$, were all present in their respective ion beams.

As for the H_2MO^- isomer, there is strong evidence for the presence of H_2PtO^- in photoelectron spectra of $[Pt(H_2O)]^-$. The peak at EBE = 3.34 eV in anion photoelectron spectrum **c** is in good agreement with the theoretically calculated EBE values of 3.40 eV and 3.45 eV. The high intensity of PtO^- in its corresponding mass spectrum, i.e., **C**, the appearance of the photoelectron spectrum of PtO^- within the mass-selected photoelectron spectrum of $[Pt(H_2O)]^-$, and the observation of H_2^+, all under relatively high source laser powers, are consistent with the presence of H_2PtO^- and with its decay into PtO^- and H_2. However, the case for the presence of H_2PtO^- at moderate source laser powers is less clear. While mass spectrum **B** exhibits PtO^-, although at relatively lower intensities than does mass spectrum **C** and while traces of H_2^+ are detected under moderate source laser power conditions, the theoretically predicted telltale H_2PtO^- peak at EBE ~3.4 eV, easily seen in photoelectron spectrum **c**, was not evident in photoelectron spectrum **b**. Instead, the EBE ~3.4 eV region in photoelectron spectrum **b** is an intensity valley, although its floor does exhibit considerable intensity. Also, the PtO^- peaks seen in photoelectron spectrum **c** are absent in photoelectron spectrum **b**. We conclude that if H_2PtO^- is formed under moderate source laser power conditions, there must be much less of it made than under higher laser power conditions. Additionally, Table I and Fig. 3 provide no significant evidence for the presence of H_2NiO^- and H_2PdO^- isomers in the beam. Also, since neither NiO^-, PdO^- nor H_2^+ were observed in $[Ni(H_2O)]^-$ and $[Pd(H_2O)]^-$ experiments, even at high source laser powers, the implication is that they were not formed.

TABLE I. Experimentally determined VDE values for $[Pt(H_2O)]^-$, $[Ni(H_2O)]^-$, and $[Pd(H_2O)]^-$ compared with the computed CCSD(T)/aug-cc-pVTZ VDE values. In the case of $[Pt(H_2O)]^-$, experimentally measured VDE values for the isomer features found in photoelectron spectrum **b** are labeled separately from that of the isomer feature found in photoelectron spectrum **c**. Experimentally determined VDE values for the hydrated-anion complexes (isomers), $Pt^-(H_2O)$, $Ni^-(H_2O)$, and $Pd^-(H_2O)$, are not included in this table.

		Theoretical VDE (eV)				Expt. VDE (eV)
$HPtOH^-$	$^2A \rightarrow {}^3A$	3.02	H_2PtO^-	$^2B_1 \rightarrow {}^3B_1$	3.45	2.98 ***b***
	$^2A \rightarrow {}^1A$	3.01		$^2B_1 \rightarrow {}^1A_1$	3.40	3.34 ***c***
	$^2A \rightarrow 2^3A$	3.70				3.83 ***b***
$HNiOH^-$	$^2A \rightarrow {}^3A$	1.81	H_2NiO^-	$^2B_1 \rightarrow {}^3B_1$	2.75	1.91
	$^2A \rightarrow {}^1A$	3.04		$^2B_1 \rightarrow {}^1A_1$	2.43	3.24
$HPdOH^-$	$^2A \rightarrow {}^3A$	2.64	H_2PdO^-	$^2B_1 \rightarrow {}^3B_1$	2.49	2.50
	$^2A \rightarrow {}^1A$	2.37		$^2B_1 \rightarrow {}^1A_1$	3.20	

High level electronic structure calculations provide insight into the reaction mechanisms and detailed rationalizations of the similarities and differences between the different metal anions. Figure 4 shows the calculated potential energy pathways and key structures involved in the reactions of Ni^-, Pd^-, and Pt^- atomic anions with a single water molecule. The coordinates and energies of these structures are provided in the supplementary material. For example, Fig. 4 provides a possible explanation for why only H_2PtO^- was formed among the three group 10 systems we studied. Figure 4 shows that only H_2PtO^- is definitively exothermic relative to $M^- + H_2O$.

Unlike the conversion of $M^+(H_2O)$ cationic complexes to $HMOH^+$ (M = Pd, Pt), which according to theory is

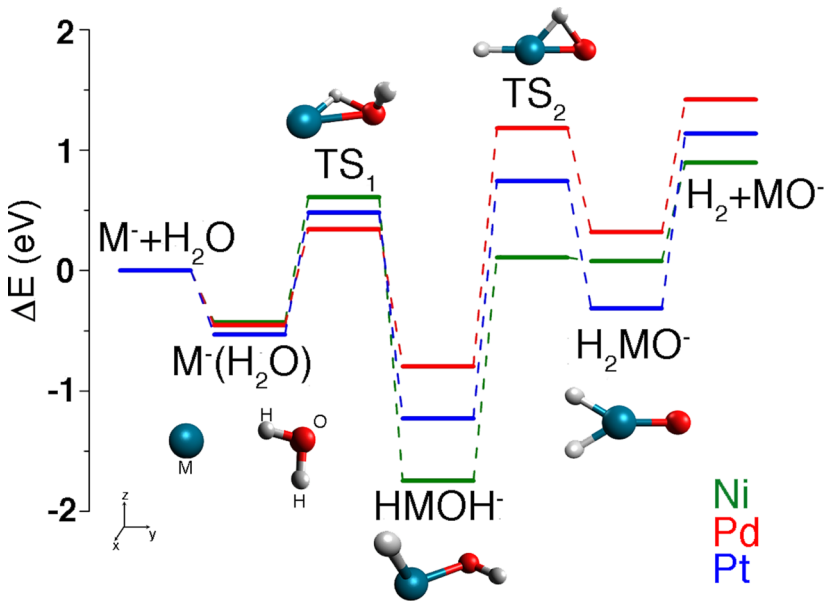

FIG. 4. The calculated potential energy pathways and stationary points involved in the reactions of Ni^-, Pd^-, and Pt^- with a single water molecule, H_2O. Zero-point vibrational and spin-orbit corrections are also included.

endothermic,[25] the transformation from $M^-(H_2O)$ anionic complexes to $HMOH^-$ is exothermic in all three (M = Ni, Pd, Pt) cases shown in Fig. 4. The transition state, TS_1, however, is higher in energy than the energies of both $M^- + H_2O$ and $M^-(H_2O)$ in all three cases. The barrier to be overcome is ~0.5 eV, i.e., the energy of TS_1 minus the energy of the reactants, $M^- + H_2O$ or ~1.0 eV, the energy of TS_1 minus the energy of $M^-(H_2O)$. These computed barriers include zero-point vibrational and spin-orbit corrections. Many reactions are known to proceed with barrier heights that are similar to these values.[26–29]

Let us further consider our results when the highest source-laser power was utilized, i.e., see panels **C** and **c** in Fig. 1. Under those circumstances, excess energy was available to the system, and in the case of H_2PtO^-, the excess energy was used to both make it and drive the reaction to the final products, PtO^- and H_2. The excess energy is also likely responsible for the formation of metastable H_2PtO^- complexes, these having been discussed above. While the origin of the excess energy that became available under these high source-laser power conditions is not fully resolved, the options are thermal excitation, electronic excitation, or both.

CONCLUSION

To summarize, we have investigated water activation and splitting by various single atomic anions, which were not previously explored in the gas phase. We demonstrated that platinum is special among all investigated metals and that a single platinum atomic anion can both activate and split a single water molecule, while single palladium and nickel atomic anions only activate water molecules.

In the electrolysis of water, H_2 gas forms at the cathode, which is typically platinum, while O_2 forms at the anode. It is interesting to contemplate the relationship between the microscopic interaction between a single platinum atom, a single electron, and a single water molecule and the more complicated, macroscopic interaction between a platinum cathode and liquid water during electrolysis. Respectively, both processes involve surmountable energy barriers and low overpotentials, which are characteristically exceptional properties of platinum.

SUPPLEMENTARY MATERIAL

See supplementary material for detailed experimental and theoretical methods and supporting experimental and theoretical results including Tables S1–S11 and Figs. S1–S11.

ACKNOWLEDGMENTS

The experimental parts of this material are based on work supported by the (U.S.) National Science Foundation (NSF) under Grant No. CHE-1664182 (KHB, Pt, Cu, Ag, and Co parts) and by the Air Force Office of Scientific Research (AFOSR) under Grant No. FA9550-15-1-0259 (KHB, Ni, Pd, Au, Fe, and V parts). The computational part of this work (S.S.X.) acknowledges support from the Center for Scalable Predictive methods for Excitations and Correlated phenomena (SPEC), which is funded by the U.S. Department of Energy, Office of Science, Basic Energy Sciences, Chemical Sciences, Geosciences and Biosciences Division, as part of the Computational Chemical Sciences Program at Pacific Northwest National Laboratory. Pacific Northwest National Laboratory (PNNL) is a multi-program national laboratory operated for DOE by Battelle. This research also used resources of the National Energy Research Scientific Computing Center, which is supported by the Office of Science of the U.S. Department of Energy under Contract No. DE-AC02-05CH11231.

The authors declare no competing financial interests.

[1] D. G. Nocera, "The artificial leaf," Acc. Chem. Res. **45**, 767–776 (2012).
[2] K. Liu, Y. Liu, N. Liu, Y. Han, S. Lee, X. Zhang, J. Zhong, H. Huang, and Z. Kang, "Metal-free efficient photocatalyst for stable visible water splitting via a two-electron pathway," Science **347**, 970–974 (2015).
[3] B. Rausch, M. D. Symes, G. Chisholm, and L. Cronin, "Decoupled catalytic hydrogen evolution from a molecular metal oxide redox mediator in water splitting," Science **345**, 1326–1330 (2014).

[4]R. J. Roach, W. H. Woodward, A. W. Castleman, Jr., A. C. Reber, and S. N. Khanna, "Complementary active sites cause size-selective reactivity of aluminum cluster anions with water," Science **323**, 492–495 (2009).
[5]M. D. Kärkäs, O. Verho, E. V. Johnston, and B. Åkermark, "Artificial photosynthesis: Molecular systems for catalytic water oxidation," Chem. Rev. **114**, 11863–12001 (2014).
[6]J. A. Kerr, "Activation of water, ammonia, and other small molecules by $PC_{carbene}P$ nickel pincer complexes," Chem. Rev. **66**, 465–500 (1966).
[7]D. V. Gutsulyak, W. E. Piers, J. Borau-Garcia, and M. Parvez, "Activation of water, ammonia, and other small molecules by $PC_{carbene}P$ nickel pincer complexes," J. Am. Chem. Soc. **135**, 11776–11779 (2013).
[8]J. Li and K. Yoshizawa, "Computational evidence for hydrogen generation by reductive cleavage of water and α–H abstraction on a molybdenum complex," Angew. Chem., Int. Ed. **50**, 11972–11975 (2011).
[9]R. Subbaraman, D. Tripkovic, D. Strmcnik, K. C. Chang, M. Uchimura, A. P. Paulikas, V. Stamenkovic, and N. M. Markovic, "Enhancing hydrogen evolution activity in water splitting by tailoring Li^+-$Ni(OH)_2$-Pt interfaces," Science **334**, 1256–1260 (2011).
[10]F. Jiao and H. Frei, "Nanostructured cobalt oxide clusters in mesoporous silica as efficient oxygen-evolving catalysts," Angew. Chem., Int. Ed. **48**, 1841–1844 (2009).
[11]J. Li, X. Wu, S. Zhou, S. Tang, M. Schlangen, and H. Schwarz, "Distinct mechanistic differences in the hydrogen-atom transfer from methane and water by the heteronuclear oxide cluster $[Ga_2MgO_4]^+$," Angew. Chem., Int. Ed. **54**, 12298–12302 (2015).
[12]S. M. Lang, T. M. Bernhardt, M. Krstic, and V. M. Koutecky, "Water activation by small free ruthenium oxide clusters," Phys. Chem. Chem. Phys. **16**, 26578–26583 (2014).
[13]X. Yang, A. Wang, B. Qiao, J. Li, J. Liu, and T. Zhang, "Single-atom catalysts: A new frontier in heterogeneous catalysis," Acc. Chem. Res. **46**, 1740–1748 (2013).
[14]N. Cheng, S. Stambula, D. Wang, M. N. Banis, J. Liu, A. Riese, B. Xiao, R. Li, T. K. Shm, L. M. Liu *et al.*, "Platinum single-atom and cluster catalysis of the hydrogen evolution reaction," Nat. Commun. **7**, 13638 (2016).
[15]C. Ling, L. Shi, Y. Ouyang, X. C. Zeng, and J. Wang, "Nanosheet supported single-metal atom bifunctional catalyst for overall water splitting," Nano Lett. **17**, 5133–5139 (2017).
[16]J. Deng, H. Li, J. Xiao, Y. Tu, D. Deng, H. Yang, H. Tian, J. Li, P. Ren, and X. Bao, "Triggering the electrocatalytic hydrogen evolution activity of the inert two-dimensional MoS_2 surface via single-atom metal doping," Energy Environ. Sci. **8**, 1594–1601 (2015).
[17]M. J. Berr, F. F. Schweinberger, M. Döblinger, K. E. Sanwald, C. Wolff, J. Breimeier, A. S. Crampton, C. J. Ridge, M. Tschurl, U. Heiz *et al.*, "Size-selected subnanometer cluster catalysts on semiconductor nanocrystal films for atomic scale insight into photocatalysis," Nano Lett. **12**, 5903–5906 (2012).
[18]K. Wu, H. Zhu, Z. Liu, W. Rodríguez-Córdoba, and T. Lian, "Ultrafast charge separation and long-lived charge separated state in photocatalytic CdS–Pt nanorod heterostructures," J. Am. Chem. Soc. **134**, 10337–10340 (2012).
[19]L. Amirav and A. P. Alivisatos, "Photocatalytic hydrogen production with tunable nanorod heterostructures," J. Phys. Chem. Lett. **1**, 1051–1054 (2010).
[20]X. Zhang, G. Liu, G. Gantefoär, K. H. Bowen, and A. N. Alexandrova, "$PtZnH_5^-$, a σ-aromatic cluster," J. Phys. Chem. Lett. **5**, 1596–1601 (2014).
[21]T. M. Ramond, G. E. Davico, F. Hellberg, F. Svedberg, P. Salén, P. Söderqvist, and W. C. Lineberger, "Photoelectron spectroscopy of nickel, palladium, and platinum oxide anions," J. Mol. Spectrosc. **216**, 1–14 (2002).
[22]J. Thogersen, L. D. Steele, M. Scheer, C. A. Brodie, R. C. Bilodean, and K. Haugen, "Electron affinities of Si, Ge, Sn and Pt by tunable laser photodetachment studies," J. Phys. B: At., Mol. Opt. Phys. **29**, 1323–1330 (1996).
[23]S. E. Eustis, D. Radisic, K. H. Bowen, R. A. Bachorz, M. Haranczyk, G. K. Schenter, and M. Gutowski, "Electron-driven acid-base chemistry proton transfer from hydrogen chloride to ammonia," Science **319**, 936–939 (2008).
[24]The fact that our mass spectra showed both PtO^- and H_{2+} as having been formed between the source and the TOF ion extractor under high source-laser power conditions also implies the formation of metastable H_2PtO^- species in the source region.
[25]O. Lakuntza, J. M. Matxain, F. Ruipérez, J. N. Ugalde, and P. B. Armentrout, "Quantum chemical study of the reactions between Pd^+/Pt^+ and H_2O/H_2S," Chem. - Eur. J. **19**, 8832–8838 (2013).
[26]A. Sanchez, S. Abbet, U. Heiz, W. D. Schneider, H. Hakkinen, R. N. Barnett, and U. Landman, "When gold is not noble: Nanoscale gold catalysts," J. Phys. Chem. A **103**, 9573–9578 (1999).
[27]H. Schwarz, "Doping effects in cluster-mediated bond activation," Angew. Chem., Int. Ed. **54**, 10090–10100 (2015).
[28]S. M. Lang, T. Bernhardt, V. Chernyy, J. M. Hakker, R. N. Barnett, and U. Landman, "Selective C–H bond cleavage in methane by small gold clusters," Angew. Chem., Int. Ed. **56**, 13406–13410 (2017).
[29]X. Zhang, G. Liu, K. H. Meiwes-Broer, G. Gantefoer, and K. H. Bowen, "CO_2 activation and hydrogenation by PtH_n^- cluster anions," Angew. Chem., Int. Ed. **55**, 9644–9647 (2016).